

Multi-Criteria Evaluation of Hybrid Solar-Ground Source Heat Pump Systems: Integrating Exergy, and Environmental Assessments[#]

Lanxiang Yang¹, Shangzhou Ma¹, Pengkun Zhou¹, Yaran Wang^{1*}

1 School of Environmental Science and Engineering, Tianjin University, Haihe Education Area, Jinnan District, Tianjin 300350, PR China

(Corresponding Author: yaran_wang@tju.edu.cn)

ABSTRACT

Solar ground source heat pump systems offer a sustainable solution that reduces energy consumption and environmental impact. This study develops an integrated solar ground source heat pump system, evaluating its exergy and environmental impacts. Results show that the exergy efficiency is 49.16%, with a total exergy destruction of 111.43 kW. The environmental impact is greatest during construction, followed by usage, disposal, and maintenance. This study provides valuable insights for optimizing renewable energy integration in building systems and serves as a guide for the design of similar energy-efficient projects.

Keywords: Solar Ground source heat pump, Exergy, Life cycle assessment

NONMENCLATURE

Abbreviations

LCA	Life cycle assessment
PVT	Photovoltaic thermal
GSHP	Ground source heat pump
SGSHP	Solar ground source heat pump

Subscripts

dep	depreciation
e	electricity
ex	exergy
m	material
ma	maintenance

1. INTRODUCTION

The expansion of renewable energy is an essential strategy to address the global energy crisis and mitigate climate change [1]. With the gradual depletion of fossil fuels and mounting environmental pressures, accelerating the development and deployment of renewables has become a worldwide priority [2]. Serving as clean and sustainable alternatives, these energy sources reduce dependence on conventional fuels, cut carbon emissions, and limit environmental pollution, thereby supporting sustainable growth and

environmental preservation [3]. The transformation of the global energy structure, coupled with the urgency of climate action, has positioned renewable energy at the forefront of future energy strategies [4]. Among renewable energy technologies, the solar ground source heat pump (SGSHP) system has attracted considerable interest in recent years for its dual capability in heating and cooling [5]. By combining the high efficiency of ground source heat pumps (GSHP) with the renewable thermal input from solar collectors, this system offers a sustainable approach that maximizes the utilization of natural resources, lowers energy consumption, and mitigates environmental impacts [6].

With the urgent need for carbon reduction and the increasing integration of renewable energy in buildings, energy conservation and efficiency are no longer the sole objectives in optimizing GSHP systems [7]. Li et al. [8] designed a double-effect absorption solar heat pump module and quantified its economic and environmental gains, achieving reductions of 10.9% in environmental impact and 3.4% in annual costs after optimization. In a life cycle assessment (LCA), Violante et al. [9] compared GSHP with ASHP systems, finding that although GSHP incurs greater impacts during manufacturing and installation, it surpasses ASHP in long-term efficiency and overall environmental performance. Eisapour et al. [10] analyzed a configuration combining a geothermal heat pump, borehole thermal energy storage, photovoltaic panels, and solar collectors, concluding that it offers superior cost-effectiveness and reliability while maintaining soil thermal balance. Chen et al. [11] developed an SGSHP system targeting carbon peak and neutrality objectives, proposing four seasonal multi-mode buried pipe partition operation schemes. Their analysis showed COP values of 3.62 in heating and 5.76 in cooling, with 9.84 tons of standard coal saved over 13 years. Chen et al. [12] conducted thermodynamic studies on a solar–geothermal hybrid system, demonstrating a

[#] This is a paper for the 5th Applied Energy Symposium and Forum: Renewable Energy Matrix (REM2025), Oct. 29-31, 2025, Yancheng, China.

COP of 6.5 and identifying optimal exergy efficiency when the ground source temperature aligns with the condenser temperature. Only a few studies comprehensively analyze and optimize SGSHP systems from the perspectives of thermodynamic performance and environmental impact.

Building on the above literature, this work develops an SGSHP system derived from a real shallow geothermal–solar collaborative project. Exergy analyses are conducted to quantify process irreversibilities and assess the system’s thermodynamic quality. In addition, a LCA is performed to examine environmental impacts. The study delivers an integrated evaluation of the SGSHP system from the perspectives of exergy and environmental performance. Distinct from prior research, the simulation and optimization are grounded in a fully operational, field-tested system, enabling direct guidance for practical operation. This approach offers both theoretical support for future system deployment and valuable insights into integrating renewable energy with building applications.

2. OVERVIEW OF THE SYSTEM

2.1 Overview of the System

Figure 1 illustrates the schematic of the coupled system, including the solar collector, thermal storage tank, plate heat exchanger, ground-coupled pipes, and heat pump. In the cooling season, heat is transferred to the soil via the shallow ground pipes. The system operates in cooling mode, activating the heat pump, source-side pump, load-side pump, and collector pump, while valves 1–3 are open and valves 4–6 remain closed.

During the transitional season, the solar collector and thermal storage tank transfer solar heat to the soil through the shallow ground pipes for thermal storage. The system runs in storage mode, with the solar collector, thermal storage tank, and plate heat exchanger active, and the heat pump and source-side pump inactive. Valves 4–8 are open, and valves 1–3 are closed.

In the heating season, heat is extracted from the soil through the shallow ground pipes. The solar collector stores heat in the thermal tank, which is then transferred via the plate heat exchanger to raise the source-side water temperature for the heat pump. The heat pump supplies heating to the end users. In this mode, the heat pump and all pumps operate, valves 1–3 and 5–8 are open, and valve 4 remains closed.

In this study, two operational modes are considered in separate simulation scenarios: Mode A, which involves

closing valves 4–8 and operating only the GSHP system, and Mode B, which entails closing valves 4 and 9 and simultaneously operating the solar collector module and the GSHP module during the transitional season.

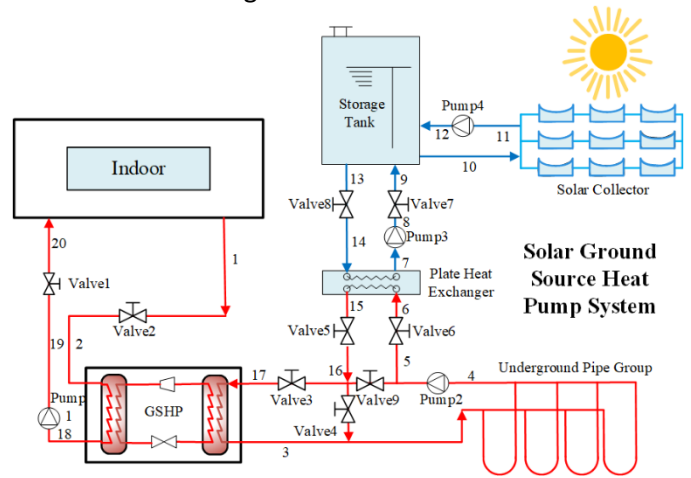


Fig. 1 Schematic of the SGSHP

2.2 System settings

The coupled system model is based on an actual shallow geothermal and solar energy project in Tianjin. The SGSHP system provides both heating and cooling for a factory covering 3913.83 m². The HVAC system is designed for a cooling load of 228.3 kW and a heating load of 157.8 kW. The shallow geothermal system comprises 100 vertical boreholes, each 120 meters deep, with a spacing of 5 meters between boreholes. Each borehole is equipped with 25 mm diameter double-U pipes, which are interconnected using high-efficiency horizontal loops arranged in series. Additionally, the system includes a screw-type GSHP to ensure efficient and reliable operation.

3. MODELING

3.1 Exergy analysis model

Exergy analysis allows for a fundamental identification of irreversibilities within a system and offers an effective method for enhancing strategies for energy cascade utilization. By considering the quality of energy exchange, exergy analysis evaluates the degradation rate of components, offering guidance for reducing exergy destruction. This method has been successfully applied to various thermodynamic processes. Exergy analysis in logistics involves evaluating three components: physical exergy (Ex_{phy}), chemical exergy (Ex_{che}), and mixed exergy (Ex_{mix}). The formula is as follows [13]:

$$Ex_{\text{phy}} + Ex_{\text{mix}} + Ex_{\text{che}} = m[(h - h_0) - T_0(s - s_0)] + \sum_{i=1}^n b_{\text{ch},i} \cdot x_i \quad (1)$$

The exergy destruction for each component is expressed as [14]:

$$ED = Ex_{\text{in}} - Ex_{\text{out}} + \sum Q(1 - \frac{T_0}{T}) + \sum W \quad (2)$$

where ED is exergy destruction, kW; W is the work done by the equipment, kW; the Ex_{in} is input exergy, kW; Ex_{out} is output exergy, kW.

Exergy efficiency (η_{ex}) is expressed as:

$$\eta_{\text{ex}} = \frac{Ex_{\text{out}}}{Ex_{\text{in}}} \quad (3)$$

Localized exergy destruction rate (φ_i) is expressed as:

$$\varphi_i = \frac{ED}{ED_{\text{total}}} \quad (4)$$

where ED_{total} is the exergy destruction of the system, kW.

3.2 Environmental analysis model

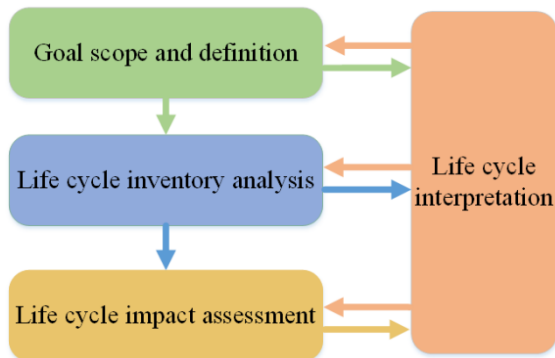


Fig. 2 Diagram of life cycle assessment boundary

Environmental assessment involves a thorough evaluation of the environmental impacts associated with coupled energy systems over their entire lifecycle. LCA is widely recognized as an essential tool for assessing the environmental benefits of renewable energy systems and guiding the sustainability of complex energy systems [15]. The LCA process is shown in Figure 2. Input resources are classified as materials and energy, whereas output includes electricity, various environmental emissions, and losses. The lifecycle is divided into four main stages: construction, usage, maintenance, and disposal.

The EI16 is adopted as the overall metric. The impact categories are divided into 22 specific indicators. The EI16 calculation formula is as follows [16]:

$$EI16 = \sum_d \sum_r dm_{br} LCI_b w_d n_{dr} \quad (5)$$

where the d and r are damage and impact categories; w_d and n_{dr} are weight and normalization factors; dm_{br} represents the damage factor; LCI_b represents the chemical in the life cycle inventory.

4. RESULTS AND DISCUSSION

4.1 Exergy analysis

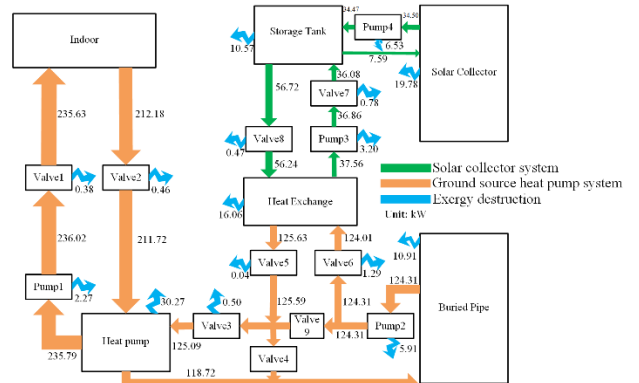


Fig. 3 Exergy diagram of the SGSHP system.

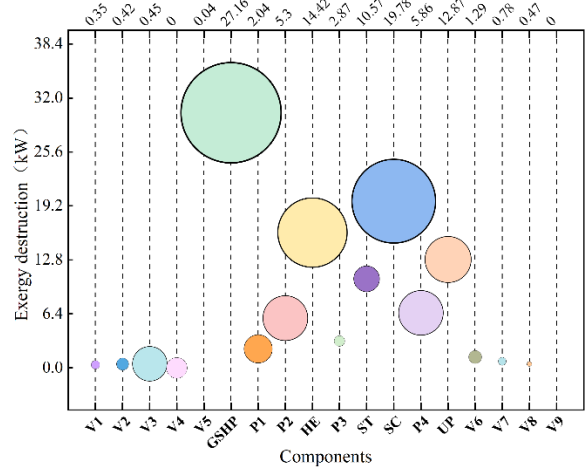


Fig. 4. Localized exergy destruction for each component

Figure 3 shows the exergy flow diagram of the SGSHP system under standard heating-season operating conditions. Figure 4 depicts the local exergy destruction across the system's components. The analysis indicates that the equipment selection is appropriate. The total exergy destruction of the system amounts to 111.43 kW, with an overall exergy efficiency of 49.16%.

The GSHP accounts for the largest share of exergy destruction in the coupled system, contributing 27.16%

of the total, equivalent to 30.27 kW. This is mainly attributed to the uneven distribution of the underground heat source, which induces significant fluctuations in the evaporator inlet temperature. These temperature fluctuations increase the average temperature difference during heat exchange, thereby raising exergy destruction. In addition, the lower outdoor temperatures during winter reduce the performance of the GSHP, resulting in higher local exergy destruction. The solar collector module ranks as the second-largest contributor to exergy destruction, accounting for 19.78% of the total, or 19.76 kW. This is primarily because the collector operates during the heating season when ambient temperatures are low, leading to exergy losses during heat transfer and resulting in significant inefficiencies in the module. The plate heat exchanger follows, with a local exergy destruction of 16.06 kW, representing 14.42% of the total destruction. This is primarily due to the large temperature difference between the hot and cold fluids, combined with uneven flow distribution, which leads to significant pressure losses, increased energy consumption, and decreased heat transfer efficiency. As a result, exergy destruction in the heat exchanger is relatively high.

Additionally, the water pumps and thermal storage tank incur irreversible exergy destruction due to pipeline resistance and heat destruction, with contributions ranging from 10.57% to 2.27%. The exergy destruction in other components are relatively small, with no component exceeding 1.29% of the total destruction. Optimizing operational parameters to improve component efficiency and minimize exergy destruction represents an effective approach to enhancing overall system performance. These aspects will be the primary targets for improvement and optimization in future system development.

4.2 Environmental analysis

Figure 5 shows the environmental impact distribution across the entire lifecycle of the SGSHP system. The construction phase has the highest EI16 value, which is $7.15E+02$, accounting for 40.04% of the total impact. The usage phase follows with an EI16 value of $6.50E+02$, making up 36.44%. The maintenance phase has an EI16 value of $8.02E+01$, contributing 4.49%, and the disposal phase has an EI16 of $3.39E+02$, which accounts for 19.03% of the overall environmental impact.

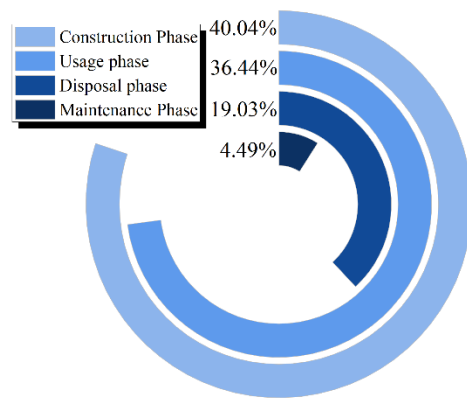


Fig5. Distribution of damage types in each lifecycle phase

The construction and operation phases exert the largest environmental impact, primarily due to energy-intensive underground pipe installation processes such as drilling and trenching, which consume substantial electricity. Additionally, producing raw materials like metals and plastics emits harmful particulates that can cause respiratory diseases. Carcinogenic substances, such as arsenic and cadmium, also have adverse health effects through air, freshwater, and soil contamination.

The usage phase of the SGSHP system consumes significant amounts of electricity, and electricity generation, in turn, consumes resources and generates emissions. In contrast, the environmental impact during the maintenance phase is minimal, with low energy consumption and reduced pollution. The four key environmental impacts—global warming potential, eutrophication, acidification, and human toxicity—show the following order of significance across lifecycle stages: construction phase > usage phase > disposal phase > maintenance phase.

The EI16 shows that the construction stage exerts the greatest environmental pressure over the system's lifecycle. Consequently, SGSHP system design plays a key role in its ecological performance. Choosing suitable equipment, adjusting component operation schedules, and varying operation across different phases and load conditions can effectively reduce environmental impacts, thereby enhancing the system's overall sustainability.

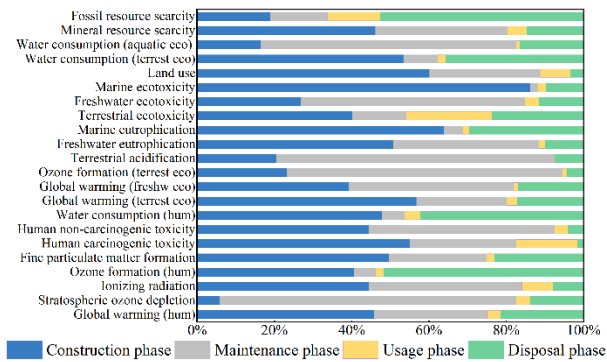


Fig6. The allocation of damage categories across each phase

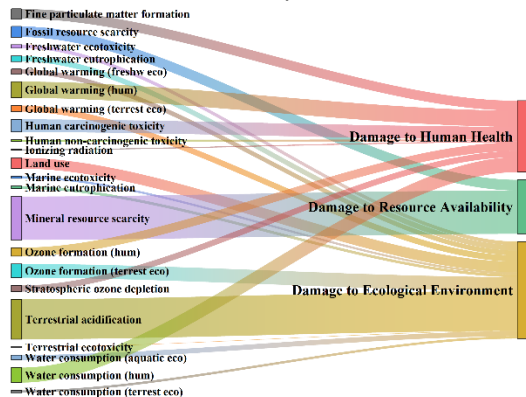


Fig7. Distribution of the three impact categories

The SGSHP system's environmental impacts differ across its lifecycle stages. Figure 6 shows the share of impacts from various categories at each stage. The 22 impact categories are normalized and grouped into three main types: human health, ecological environment, and resource availability. Figure 7 presents the distribution of these aggregated categories. In the construction stage, human health impacts represent 42.91%, mainly stemming from pollutant emissions during metal production, such as fine particulate matter and toxic compounds. These pollutants pose significant risks to the respiratory system and increase the likelihood of diseases such as cancer. Ecological environmental damage constitutes 38.76%, primarily stemming from the emissions of sulfur dioxide and nitrogen oxides, as well as the extensive consumption of fossil fuels during electricity and raw material production.

During the usage phase, ecological impacts dominate, representing 57.96% of the total. This is mainly caused by the system's high water consumption, which can result in resource waste and pollution, directly affecting local freshwater ecosystems. Additionally, the operation of the GSHP may lead to thermal pollution in surrounding freshwater environments, adversely affecting aquatic life and biodiversity. The environmental impact distribution in the maintenance phase is similar to the construction phase but differs slightly, with

ecological damage accounting for 20.54%. This impact arises from pollutant emissions during electricity generation and the environmental effects of maintenance material production. In the decommissioning stage, ecological impacts are predominant, accounting for 51.68% of the total. This mainly arises from metal recycling processes, while the disposal of inert waste in landfills adds further environmental pressure.

To mitigate the adverse effects of the SGSHP system on various ecosystems during the construction and usage phases, a series of effective management and control strategies must be implemented. These strategies should include optimizing water resource management to reduce unnecessary water consumption and potential contamination, strengthening soil thermal balance monitoring to maintain stable and appropriate soil temperatures, thus safeguarding the health of the soil ecosystem, and actively protecting surface vegetation to prevent irreversible damage during installation and usage. In the preliminary planning and design phase of the SGSHP system, it is crucial to accurately assess the actual conditions of the low-temperature heat source to provide a solid foundation for subsequent design and deployment. When meeting specific user demands, efforts should be made to set lower outlet temperatures to help maintain efficient system operation, thereby reducing energy consumption and improving overall environmental performance.

5. CONCLUSIONS

This study presents an integrated solar-ground source heat pump system based on a shallow geothermal and solar. Models for exergy and environmental impact were developed to evaluate the system. Simulations and optimizations using actual operational data provide guidance for system operation. The main conclusions are:

- 1) With the total exergy destruction for the entire system calculated at 111.43 kW, yielding an exergy efficiency of 49.16%. Among the components, the GSHP is identified as the primary contributor to the exergy destruction of system, accounting for 27.16% of the total exergy destruction, or 30.27 kW. While the equipment selection for the system is considered reasonable, potential improvements in system performance and environmental efficiency could be achieved through measures such as reducing the collector area and optimizing the mounting angle.

- 2) The order of the impact of each phase of the life cycle on the environment is: construction phase > usage

phase > disposal phase > maintenance phase. The EI16 for the construction phase is 7.15E+02, accounting for 40.04% of the total; for the usage phase, EI16 is 6.50 E+02, representing 36.44%; for the maintenance phase, EI16 is 8.02 E+01, contributing 4.49%; and for the disposal phase, EI16 is 3.39 E+02, accounting for 19.03%.

ACKNOWLEDGEMENT

The authors are grateful for the financial support provided by the China National Key R&D Program [Grant No.2020YFD1100305-02].

REFERENCE

[1] Saher, S, Johnston, S, et al. Trimodal thermal energy storage material for renewable energy applications [J]. *Nature* 636, 622–626 (2024).

[2] Gallo M, Marrasso E, Martone C, et al. Energy, economic and environmental benefits of a car-sharing system with electric vehicles integrated into a renewable energy community [J]. *Sustainable Energy Technologies and Assessments*, 2025, 81: 104428.

[3] Du J, Liu Y, Xu Z, et al. Global effects of progress towards Sustainable Development Goals on subjective well-being[J]. *Nature Sustainability*, 2024, 7(3): 360-367.

[4] Haider S M A, Ratlamwala T A H, Kamal K, et al. Integrated energy, exergy, and environment (3E) analysis, and life cycle assessment of renewable sourced multigeneration system for optimized performance and environmental impact assessment[J]. *Sustainable Energy Technologies and Assessments*, 2025, 80: 104368.

[5] Gao J, Li S, Wu F, et al. Study on efficient heating method by solar coupled air source heat pump system with phase change heat storage in severe cold region [J]. *Applied Energy*, 2024, 367: 123206.

[6] Qiu G, Li K, Cai W, et al. Optimization of an integrated system including a photovoltaic/thermal system and a ground source heat pump system for building energy supply in cold areas [J]. *Applied Energy*, 2023, 349: 121698.

[7] Yin L, Tao M. Balanced broad learning prediction model for carbon emissions of integrated energy systems considering distributed ground source heat pump heat storage systems and carbon capture & storage [J]. *Applied Energy*, 2023, 329: 120269.

[8] Li H, Bi Y, Wang H, et al. Multi-objective optimization of an absorption solar-ground source heat pump considering the environmental and economic performance [J]. *International Journal of Green Energy*, 2023, 20(11): 1177-1190.

[9] Violante A C, Donato F, Guidi G, et al. Comparative life cycle assessment of the ground source heat pump vs air source heat pump [J]. *Renewable Energy*, 2022, 188: 1029-1037.

[10] Wen Y, Lau S K, Leng J, et al. Sustainable underground environment integrating hybrid ventilation, photovoltaic thermal and ground source heat pump [J]. *Sustainable Cities and Society*, 2023, 90: 104383.

[11] Eisapour A H, Rad F M, Fung A S. Techno-economic and environmental study of a hybrid solar ground source heat pumps for a heating-dominated community in a cold climate; a case study in Toronto [J]. *Renewable Energy*, 2024, 231: 120874.

[12] Chen P, Xu Y, Ning H, et al. Performance of a solar ground source heat pump used for energy supply of a separated building [J]. *Geothermics*, 2022, 105: 102524.

[13] Chen L, Yue H, Wang J, et al. Thermodynamic analysis of a hybrid energy system coupling solar organic Rankine cycle and ground source heat pump: Exploring heat cascade utilization [J]. *Energy*, 2023, 284: 129228.

[14] Xu A, Yang L, Huang W, et al. Exergy, economic, exergoeconomic and environmental (4E) analyses and multi-objective optimization of a PEMFC system for coalbed methane recovery [J]. *Energy Conversion and Management*, 2023, 297: 117734.

[15] Kelly S, Tsatsaronis G, Morosuk T. Advanced exergetic analysis: Approaches for splitting the exergy destruction into endogenous and exogenous parts [J]. *Energy*, 2009, 34(3): 384-391.

[16] Xu A, Yang L, Song T, et al. A cascade lithium bromide absorption refrigeration/dehumidification system for efficient energy recovery: Development, 3E optimization and life cycle assessment [J]. *Journal of Cleaner Production*, 2023, 383: 135286.